UNSYS digital

Journal of Unmanned System Technology

Control of an Unmanned Underwater Vehicle using An Optimized LQR Method

Ismaila B. Tijani[†] and Agus Budiyono[‡]

[†]Electronics Engineering, ADMC, HCT, United Arab Emirates

[‡]School of Engineering, Aerospace & Aviation Program, RMIT University, Melbourne, Australia

Abstract— This paper presents an optimal control synthesis for an unmanned underwater vehicle using a Multiobjectives Differential Evolution (MODE)-based LQR approach. Although the LQR control is a well-known optimal control method, the optimality of the resulting compensator is a subject of appropriate design parameters' (Q and R) selection. Considering the complex dynamics nature of an unmanned underwater vehicle, and the need to achieve optimal compromise between several control performance objectives such as time response, control energy minimization and robustness, the conventional LQR design approach is not only potentially challenging, it is time consuming and limits the achievable performance. In this paper, the control problem is formulated as a Multiobjectives optimization problem to search for Pareto-based optimal (sub-optimal) design parameters using a MODE-algorithm. The performance evaluation of the resulting compensator in simulation shows an effective compromise between the conflicting performance objectives, while the design approach is observed to be effective in rapid prototyping and deployment of such vehicle.

Keywords— LQR, optimal control, Multiobjectives Differential Evolution, optimization.

DOI: 10.21535/just.v7i1.1038

I. INTRODUCTION

THE interest in an unmanned underwater vehicle (UUV) is attributed to its current and numerous potential applications in marine-based activities such as underwater installation inspection and repairs work by offshore company, oceanographic data collection, observation of sea floor or sea bed, examination of water composition, underwater military surveillance and rescue etc. [1]. Apart from states estimation and mission plan algorithm, deployment of such vehicle either as a remotely operated vehicle (robot) (ROV) or as fully autonomous underwater vehicle (AUV) required an effective guidance and control system (GCS). Several control techniques have been reported in the literatures for GCS development [[2]-[4]]. By neglecting coupling among the system states, classical SISO-based approach such as PID and Fuzzy-PID have been applied as reported in [[5]-[7]]. Apart from lack of robustness problem, the limitation of these SISO-based approaches lies in their inability to handle effect of coupling among the states, hence limit the operational range of application. To achieve better robustness and handling coupling in the system dynamics, MIMO-based techniques such as LQR/LQG [[8]-[9]], H_∞ robust control, [[10]-[11]] and intelligent control approach using neural network [[12]-[14]] have been reported. Considering the LQR optimal control approach, it is a bridging technique and a mid-way choice between the classical SISO based control and the modern MIMO-based control techniques from the point of view of simplicity of design, implementation versus performance objectives. The literatures revealed that LQR provides better performance over classical control scheme such as PID though with higher design and implementation complexity. On the other hand, it represents the simplest model-based MIMO controller in terms of design and implementation when compared to others such as H-infinity, μ-synthesis and nonlinear controllers [[15]-[16]]. However, LQR control is a well-known optimal control method, the optimality of the resulting compensator is a subject of appropriate design parameters' (Q and R) selection [17]. However, one of the common challenges associated with LQR and generally with the majority of the modern control techniques is their dependency on selection of appropriate design parameters. Although there exists a general guideline on the choices of the form of *Q* and *R* with respect to the quadratic cost function to be minimized in the design procedure, there is no particular information on the selection of the parameters of both matrices. The selection is usually based on technical guess followed by several iterative tunings which are mostly based on trial and error for a given problem, [18]. Considering the complexity and dimension of the underwater vehicle, this conventional trial and error design approach would be time consuming in proportionate with experience of the designer, and often limits the achievable control performance objectives which are usual conflicting. In order to overcome this, the control problem is formulated as a Multiobjectives optimization task, and a proposed Multiobjectives differential Evolution algorithm proposed in [19] is applied to achieve an optimal/sub-optimal compromise between the performance objectives.

The rest of the paper is organized as follows. Next section presents the system description and mathematical modeling.

Corresponding author: Agus Budiyono (e-mail: agus.budiyono@rmit.edu.au)

This paper was submitted on December 1, 2015; revised on December 21, 2015; and accepted on December 26, 2015.

The theory of LQR control method, proposed optimized design approach and application to UUV control are given in Section **Error! Reference source not found.**. Results, discussion and analysis are given in Section **Error! Reference source not found.**, while the paper is concluded in Section V.

II. System Description and Modelling

A biological-inspired squid-like AUV structure developed at ITB [20] is adopted as test bed in this study. Figure 1 shows the AUV system with both fixed earth inertial coordinate frame, {E} and the moving body coordinate frame, {B} describing the system's coordinate of motion. Based on the kinematics of the system motion, the moving frame, {B} located at the center of gravity of the system, is described by six velocity components, $[u(t), v(t), w(t), p(t), q(t), r(t)]$ while the frame,{E} consists of six position components, $[x(t), y(t), z(t), \phi(t), \theta(t), \psi(t)]$. The descriptions of these components of motion in both reference frames are given in Table 1.

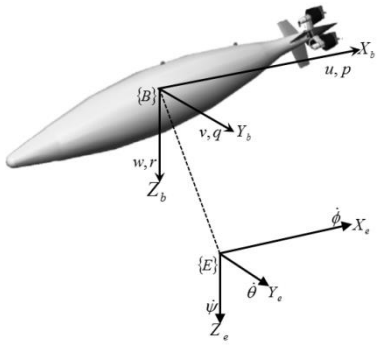

Figure 1 A squid-like Autonomous Underwater (AUV) [20]

Table 1 Components of the system motion in inertial body and earth fixed reference frames

Components in Body Frame, {B}	Components in Earth reference frame, {E}
$u_{(t)}$ translational velocity in *x*-axis	$x_{(t)}$ translation position in *x*-axis
$v_{(t)}$ translational velocity in *y*-axis	$y_{(t)}$ translation position in *y*-axis
$w_{(t)}$ translational (heave) velocity in *z*-axis	$z_{(t)}$ translation position in *z*-axis
$p_{(t)}$ angular velocity in *x*-axis	$\phi_{(t)}$ angular rotation in *x*-axis
$q_{(t)}$ angular velocity in *y*-axis	$\theta_{(t)}$ angular rotation in *y*-axis
$r_{(t)}$ angular (yaw rate) in *z*-axis	$\psi_{(t)}$ angular rotation in *z*-axis

The two frames are related through the following transformation expression:

$$\Gamma = \begin{bmatrix} p \\ q \\ r \end{bmatrix} = \begin{bmatrix} 1 & 0 & -\sin\theta \\ 0 & \cos\phi & \sin\phi\cos\theta \\ 0 & -\sin\phi & \cos\phi\cos\theta \end{bmatrix} \begin{bmatrix} \dot{\phi} \\ \dot{\theta} \\ \dot{\psi} \end{bmatrix} \quad \textbf{(1)}$$

Apart from the kinematic equation in (1), the rigid body equation of motion of the UUV is obtained by contribution of forces and moments due to: (i) inertial, (ii) gravity and buoyancy, (iii) added mass, (iv) propulsion, (v) steady-states, and (vi) control.

The detailed derivation of the system governing equations is reported in [20], while the brief summary is given here for the longitudinal dynamics considered in the control application.

A. Contributing Forces and Moments

In general, the total forces and moments acting on the UUV can be written as:

$$\begin{aligned} F &= F_{G-B} + F_{added\,mass} + F_{ss} + F_{prop} + F_{cont} \\ M &= M_{G-B} + M_{added\,mass} + M_{ss} + M_{prop} + M_{cont} \end{aligned} \quad \textbf{(2)}$$

The inertial forces and moments are derived from the Euler-Newton equation:

$$F = \frac{d}{dt}(mU_o) \quad \textbf{(3)}$$

Assuming constant mass, and evaluate the forces with respect to the body frame which moves with respect to the inertial frame, the expression (2) becomes:

$$F = m\left(\left(\frac{dU_o}{dt}\right)_{xyz} + \Gamma + U_o + \frac{d\Gamma}{dt} \times r_G + \Gamma \times (\Gamma \times r_G)\right) \quad \textbf{(4)}$$

where is U_o is the velocity vector, r_G is the position vector of vehicle center of gravity with respect to the body axis. The forces equation in (4) can be decomposed into three scalar components:

$$\begin{aligned} X &= m\left[\dot{u} + wq - vr - x_G\ q^2 + r^2\ + y_G\ pq - \dot{r}\ + z_G\ pr + \dot{q}\ \right] \\ Y &= m\left[\dot{v} + ur - wp - y_G\ r^2 + p^2\ + z_G\ qr - \dot{p}\ + x_G\ qp + \dot{r}\ \right] \\ Z &= m\left[\dot{w} + vp - uq - z_G\ p^2 + q^2\ + x_G\ rp - \dot{q}\ + y_G\ rp + \dot{p}\ \right] \end{aligned} \quad \textbf{(5)}$$

Similarly, the moment's equations are given as:

$$\begin{aligned} M_x &= p\int_\nabla y^2 + z^2\ dm - q\int_\nabla xydm - z\int_\nabla xzdm \\ M_y &= -p\int_\nabla xydm + q\int_\nabla z^2 + x^2\ dm - r\int_\nabla yzdm \\ M_z &= -p\int_\nabla xzdm - q\int_\nabla yzdm + r\int_\nabla x^2 + y^2\ dm \end{aligned} \quad \textbf{(6)}$$

The forces and moments due to gravity and buoyancy represents hydrostatic forces and moments acting on the vehicle. Expressed in the body frame, they are given as:

$$F_{G-B} = g\ m - \rho\nabla\ -\sin\theta i + \sin\phi\cos\theta j + \cos\phi\cos\theta k \quad \textbf{(7)}$$

$$\begin{aligned} M_{G-B} = g\ & my_G - \rho\nabla y_B\ \cos\phi\cos\theta - mz_G - \rho\nabla z_B\ \sin\phi\cos\theta\ i \\ & - mz_G - \rho\nabla z_B\ \sin\theta + mx_G - \rho\nabla x_B\ \cos\phi\cos\theta\ j \\ & - mx_G - \rho\nabla x_B\ \sin\phi\cos\theta + my_G - \rho\nabla y_B\ \sin\theta\ k \end{aligned} \quad \textbf{(8)}$$

The added mass forces and moments are due to hydrodynamic force due to acceleration of the vehicle. Generally the added mass is given in terms of tensor with elements A_{ij}, representing the magnitude of the added mass in the *i*-direction due the acceleration in the *j*-direction. The value of *i,j* from 1 to 3 represents the masses associated with surge, sway and heave motion, while those from 4 to 6 represents the moment of inertias associated with roll, pitch and yaw motion.

In terms of the equivalent derivative coefficients, the forces and moments are given as:

$$Added\,mass = -\begin{bmatrix} X_u & 0 & 0 & 0 & 0 & 0 \\ 0 & Y_v & 0 & 0 & 0 & N_v \\ 0 & 0 & Z_w & 0 & M_w & 0 \\ 0 & 0 & 0 & K_p & 0 & 0 \\ 0 & 0 & Z_q & 0 & M_q & 0 \\ 0 & Y_r & 0 & 0 & 0 & N_r \end{bmatrix} \quad (9)$$

The steady state forces and moments are the result of the viscous fluid effect and are usually calculated based on semi-empirical (empirical) formula or model testing. Using multivariate Taylor series expansion around the equilibrium point, the forces and moments are assumed to be function of velocity as follows:

$$\begin{aligned} X_s\ U_o + u^*, v, w, p, q, r\ = X_o + & \left(u\frac{\partial}{\partial u} + v\frac{\partial}{\partial v} + w\frac{\partial}{\partial w} + \right. \\ & \left. p\frac{\partial}{\partial p} + q\frac{\partial}{\partial q} + r\frac{\partial}{\partial r} \right) X_o \\ & + \frac{1}{2!}\left(u\frac{\partial}{\partial u} + v\frac{\partial}{\partial v} + w\frac{\partial}{\partial w} + \right. \\ & \left. p\frac{\partial}{\partial p} + q\frac{\partial}{\partial q} + r\frac{\partial}{\partial r} \right)^2 X_o \\ & + \ldots \end{aligned} \quad (10)$$

where $X_o = X_s(U_o, 0,0,0,0,0)$, and

$$\left(u\frac{\partial}{\partial u} + v\frac{\partial}{\partial v} + w\frac{\partial}{\partial w} + \cdots \right)^2 = u^2\frac{\partial^2}{\partial u^2} + v^2\frac{\partial^2}{\partial v^2} + w^2\frac{\partial^2}{\partial w^2} + \cdots \quad (11)$$

The propulsion forces and moments: are due to the UUV propeller-based thrusters. In the Squid-like vehicle, the thrust (*T)*, is function of velocity (U_A), the number of blade (n), fluid density (ρ), and propeller diameter (D):

$$T = \rho\ n^2 D^4 \tau_o + nD^3 \tau_1 U_A + D^2 \tau_2 U_A^2 + \frac{D\tau_3}{n} U_A^3 \quad (12)$$

and the propulsion forces and moments can be calculated as:

$$\begin{aligned} X_p &= \sum 1 - t_i\ T_i \cos\ \varepsilon_i \\ X_z &= \sum 1 - t_i\ T_i \sin\ \varepsilon_i \\ M_p &= X_p z_p \end{aligned} \quad (13)$$

where $U_A = u - uw$.

The control forces and moments the UUV Squid is control by three differential thrust, $[T_1, T_2, T_3]$, from three different thrusters. Table 2 gives the description of the thruster control for the longitudinal mode. Thruster 2 and 3 can be used simultaneously for the longitudinal mode maneuver, while for the pitch-up or pitch-down maneuver, all three thrusters can also be used simultaneously.

Table 2 Thruster Control for the Longitudinal Mode

Thruster	Maneuver	Control Input
T_1	Pitch up	reduction of thrust, $-\delta T_1$
	Pitch down	Increase of thrust, $+\delta T_1$
T_2, T_3	Pitch up	Increase of thrust, $+\delta T_{2,3}$
	Pitch down	Reduction of thrust, $-\delta T_{2,3}$

Each thrust can be expressed as:

$$T_i = T_{oi} + \delta T_i \quad (14)$$

In this case, the propulsion force can be expressed as:

$$\begin{aligned} X_p = \sum X_{p_i} &= \sum 1 - t_i\ \ T_{oi} + \delta T_i \\ &= \sum 1 - t_i\ T_{oi} + \sum 1 - t_i\ \delta T_i \end{aligned} \quad (15)$$

Therefore, the control force and moment are written as:

$$\begin{aligned} X_c &= \sum 1 - t_i\ \delta T_i \\ &= 1 - t\ \delta T_1 + 1 - t\ \delta T_2 + 1 - t\ \delta T_3 \end{aligned} \quad (16)$$

$$\begin{aligned} M_c &= \sum 1 - t_i\ \delta T_i z_{p_i}, \qquad i = 1,2,3 \\ &= 1 - t\ \delta T_1 z_{p_1} + 1 - t\ \delta T_2 z_{p_2} + 1 - t\ \delta T_3 z_{p_3} \end{aligned} \quad (17)$$

B. Linearized model for the longitudinal dynamics

Combining the above expression for forces and moments, the linearized model of the longitudinal dynamics of the system around operating point of speed, $U_0 = 1.5\ m/s$ and depth variation, $D = 50\ m$ is given as:

$$\dot{\bar{x}} = A\bar{x} + B\bar{\delta} \quad (18)$$

where the state vector, $\bar{x} = \{u, v, w, \theta\}$, and the control vector, $\bar{\delta} = \{\delta T_1, \delta T_2, \delta T_3\}$. For the above operating points, the system dynamic matrices A and B are given as [2]:

$$A = \begin{bmatrix} -0.6122 & 0 & 0 & 0.2935 \\ -0.0019 & -0.5633 & 0.1113 & 0.0066 \\ 0.0570 & 2.4393 & -0.4531 & -0.2014 \\ 0 & 0 & 1 & 0 \end{bmatrix} \quad (19)$$

$$B = \begin{bmatrix} 1.669225E-03 & 1.669225E-03 & 1.669225E-03 \\ 8.90925E-06 & -1.92728E-06 & -1.92728E-06 \\ -2.73863E-04 & 5.9243E-05 & 5.9243E-05 \\ 0 & 0 & 0 \end{bmatrix} \quad (20)$$

This dynamic model is used in the next section for the synthesis of the optimal control proposed in this study, which invariably can be extended to the full system model.

III. Optimized LQR Control Formulation and Application

Given a linear time invariant (LTI) state-space model of the system as described in Section II, equation (20), the goal of the LQR full-state feedback control approach is to compute the feedback gains K_{lqr} that minimizes the quadratic cost function, *J*, given as:

$$J = \int_0^\infty (\hat{x}^T Q \hat{x} + \delta^T R \delta) \quad (21)$$

The control law to achieve (21) satisfies the Algebraic Riccati Equation (ARE) and is given as:

$$\delta = -K_{lqr}x \tag{22}$$

where $K_{lqr} = R^{-1}B^{\mathrm{T}}P$, the matrices Q and R are symmetric positive semi definite and positive definite weighting matrices, respectively.

Matrices Q and R are the main design parameters to be selected by the designer to satisfy the desired control objectives. In general as indicated in Equation (21), the matrices affect the achievable performance in the following ways [[17]-[18]].

i. Q and R regulates both the states, x, and control input, δ respectively to be as small as possible. Larger values of R penalize $u$by making it smaller compare to x, while lager values of Q penalize x by making its smaller compare to δ. A trade-off is often required between the achievable minimization of states against the desired minimization of the control input.

ii. Q and R matrices also affect the position of the close-loop poles, hence, selection of Q and R affects indirectly the achievable time-domain responses/performances of the resulting close-loop system.

Therefore, the choice of Q and R greatly influence the success of the LQR controller synthesis. More so, with the availability of many of software to solve the required Riccati optimal equations involved in the computation of the LQR gains, the major design effort in the controller synthesis has been on the tuning of the weighting matrices for a given system.

A. *Optimization problem formulation*

The optimization problem is to determine the set of decision vectors, Φ, which in this context is the weighting matrices Q and R's parameters:

$$\Phi := [\Phi_1 \ldots \Phi_{\hat{n}+m}]$$

that minimizes the cost function:

$$\hat{J} = \int_0^{\infty} \hat{x}^T Q \hat{x} + \delta^T R \delta \; dt$$

and set of performance objectives of size Ω:

$$\begin{gathered} \min_{\Phi} f_i \;\; \Phi \;\; , i = 1,2,\ldots,\Omega \\ \text{subject to } Q \geq 0 \text{ and } R > 0, \text{with } 0 < \Phi_j < H_j \end{gathered} \tag{23}$$

where H_j is the upper bound on the decision parameter Φ_j.

As stated in (23), the problem is casted as non-constraint optimization problem, meanwhile, depends on design goal and application requirements, it is possible to introduce additional constraints such as frequency response parameters or actuator limitation. Figure 2 shows the proposed design method.

Experience reveals that for a given system, several iterations are required to obtain satisfactory performances depending on the dimension and complexity of the problem under consideration. In order to address this problem, a Multi-objectives differential evolution algorithm (MODE) proposed in [19] is adopted to achieve an optimized-LQR design approach. Detailed presentation of the MODE algorithm and its application to control synthesis can be obtained in [19]-[20],[22].

As shown in the Figure 1, the performance objective function is given by the response of the full-state feedback system formed for a given decision parameter set. In this study, five control Objective functions are defined for the pitch angle tracking control as follows:

$$f_i(\Phi) := \left[t_s^{(\theta)},\; OS^{(\theta)},\; {}_{\max}t_s^{u,w,q},\; {}_{\max}\beta^{u,w,q},\; {}_{\max}\delta \right] \tag{24}$$

where $t_s^{(\theta)}$ and $OS^{(\theta)}$ are the settling time and percentage overshoot of the pitch angle θ, respectively. ${}_{\max}t_s^{(u,w,q)}$ is the maximum off-axis (other states $\{u, v, w\}$) settling time, ${}_{\max}\beta_s^{(u,w,q)}$ is the maximum peak of the off-axis response, and ${}_{\max}\delta$ is the maximum control signal expended.

B. *Application to the UUV system*

For a tracking and regulation control problem as shown in the Figure 2, the system states are first augmented with two extra integral states vector to improve the tracking performance. The new state vector $\bar{x}_i$ is given as:

$$\bar{x}_i := \left[u, \quad q, \quad w, \quad \theta, \quad \int_0^t \theta \, d\tau \right] \tag{25}$$

The augmented state space model is then expressed as:

$$\dot{\bar{x}}_i = A_i \hat{x}_i + B_i \delta \tag{26}$$

and the control law becomes:

$$\bar{\delta}_i = -K_i \bar{x}_i \tag{27}$$

A_i and B_i are:

$$A_i = \begin{bmatrix} A & 0_{3\times 1} \\ \begin{bmatrix} 0_{1\times 3} & 1 \end{bmatrix} & 0 \end{bmatrix}, \quad B_i = \begin{bmatrix} B \\ 0_{1\times 3} \end{bmatrix} \tag{28}$$

Hence, $Q \in \Re^{n_i \times n_i}$, $R \in \Re^{n_i \times n_i}$ and the decision vector $\Phi \in \Re^{n_i+m}$.

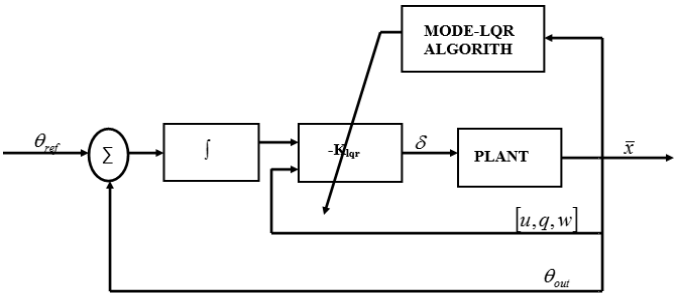

Figure 2 Block diagram of the proposed MODE-Based LQR Control Synthesis

As indicated in Figure 2, the design procedure involves placing the MODE in the LQR conventional design loop for

optimal tuning of the Q and R matrices, and can be summarized step-wise as follows:

Step 1: specify the optimization parameters: population size, *NP*, decision vector size, *Z*, DE cross-over constant, *CR* and generation size, *GEN*.

Step 2: specify the dimension of the Q and R matrices and initialize population *P* of size *NP* for the Q and R matrices' parameters.

Step 3: test for the positive definiteness of the initialized matrices, and removed any unfit parameters set(s), repeat step 2 to complete the size of population.

Step 4: Compute the objective function and extract the objectives vector Π for the population.

Step 5: Start the optimization process: while the stopping criteria is untrue, *e.g.* while $k \leq GEN$, repeat steps 6 to 9; else go to step 10.

Step 6: generate new child vector from randomly selected three vectors from the old population using the DE operation of mutation and cross over-processes. Test the positive definiteness of the child vector and compute its objective function.

Step 7: compete the child vector with parent vector for Pareto dominance. That is, determined if the child vector dominates the parent vector. If no, repeat step 6 to 7, else proceed to step 8

Step 8: update the new population with the dominant child vector

Step 9: compute the stopping criteria and update the generation count: $k = k + 1$.

Step 10: stop the optimization and report the Pareto-dominance candidates.

Five non-dominated controller candidates are selected out of the final non-dominated candidates based on Pareto-concept. Table 3 and Table 4 show the selected controller candidates and their corresponding performance objectives, respectively. The comparative response of the five controllers (K1, K2, K3, K4, and K5) is shown in Figure 3.

As shown in the Table 4, all the five candidates are potential sub-optimal controller for the system. The final choice is left to practical judgment of the designer which may be based on overall priority on the control objective. A decision matrix is proposed in [20] to guide in the final choice among the Pareto-solutions candidates. In this study, candidate K5 is selected for further performance analysis as described in the next section.

Table 3 Decision parameters of five selected controller candidates

Φ_1	Φ_2	Φ_3	Φ_4	Φ_5	Φ_6	Φ_7	Φ_8
46.302	8.781	48.855	23.107	0.000	3.783	23.206	0.000
1.539	32.508	0.514	62.443	141.286	25.424	3.636	3.749
97.864	29.750	87.318	86.111	0.460	0.000	0.001	1.841
98.854	8.143	4.538	93.365	0.771	0.000	0.001	84.828
85.796	48.178	94.167	73.600	97.757	3.063	2.909	2.867

Table 4 Performance objectives of the five controller candidates

$t_s^{(\sigma)}$	$OS^{(\sigma)}$	$\max t_s^{(u,w,q)}$	$\max \beta^{(u,w,q)}$	$\max \delta$
57.5996	0.1196	56.0273	0.0570	36.7466
75.7862	0.1400	88.7769	0.0595	0.2982
35.8344	0.0872	45.0206	0.0497	36.3085
34.0275	0.0791	35.2111	0.0510	53.8451
75.7704	0.1399	88.4696	0.0595	0.2682

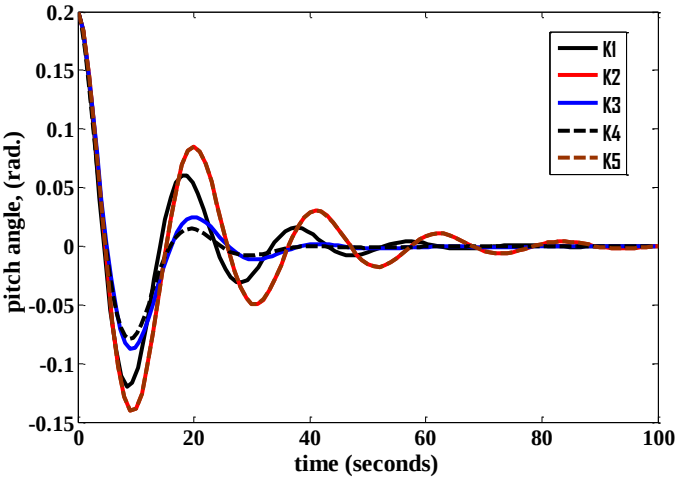

Figure 3 Responses of the five Pareto-controllers to 0.2 rad regulator input

IV. Results and Discussion

A MATLAB-Simulink model of the UUV is developed for performance analysis of the optimized-LQR controller as shown in Figure 4. Firstly, the tracking performance of the compensator with 0.2 rad, 2 kHz square pitch angle command with the nominal plant model is examined. Figure 5 shows the response of the pitch angle, forward velocity, pitch rate and vertical velocity, respectively.

Secondly, the performance of the compensator in the face of both disturbance (in forward velocity) input (ocean wave) and sensor noise is evaluated. The disturbance V_w is generated based on the following expression, [23]:

$$V_w = \Gamma_{wind}(\mu, \sigma^2) + a\sin(\omega_w t) \quad \textbf{(29)}$$

where $\Gamma_{wind}(\mu, \sigma^2)$ is stochastic process representing the wind turbulence defined by white noise with mean, $\mu = 0$ and variance, $\sigma^2 = 0.7$, while the sinusoidal term represent the wind

gust with amplitude $a = 3.3$ ft/s and frequency $\omega_w = 0.628$ rad/s. The sensor noise on the other hand is simulated with Gaussian random signal with variance of 0.7. The disturbance input and the sensor noise generated are shown in Figure 6. Figure 7 shows comparatively the pitch angle, pitch rate, forward velocity and vertical velocity responses with and without the noise and disturbance input.

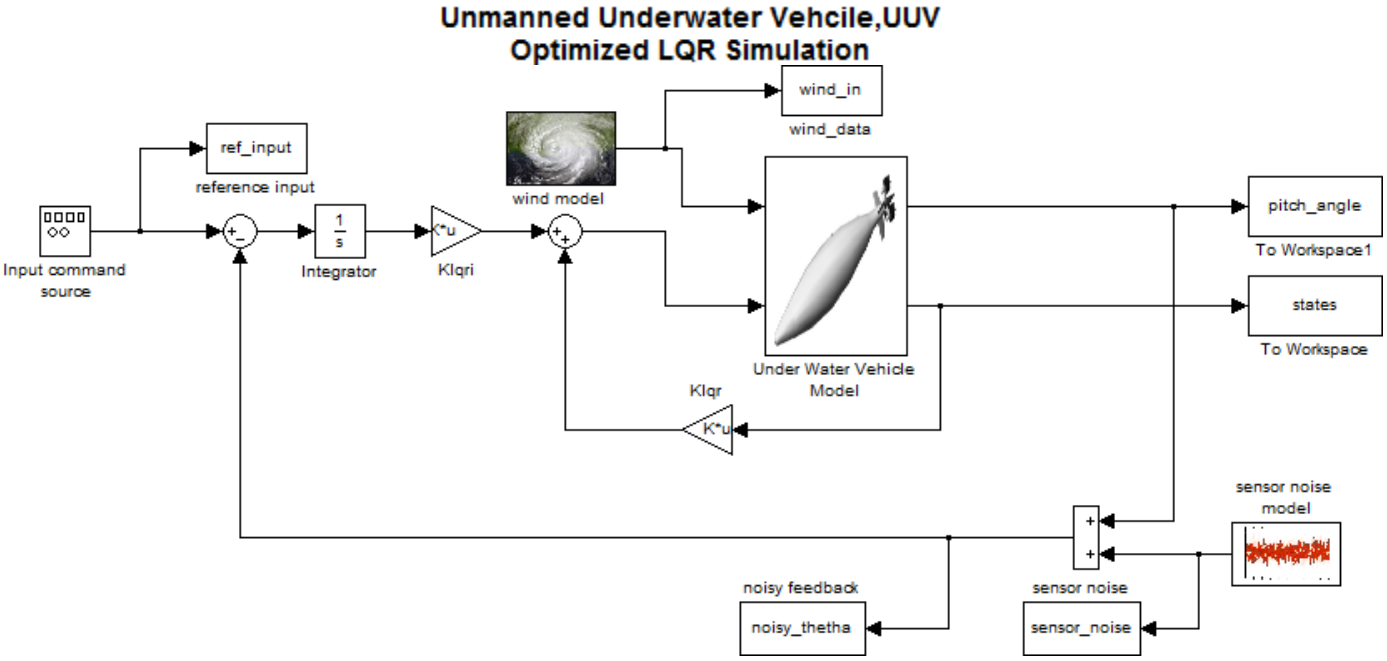

Figure 4 MATLAB-Simulink model for the controller performance evaluation

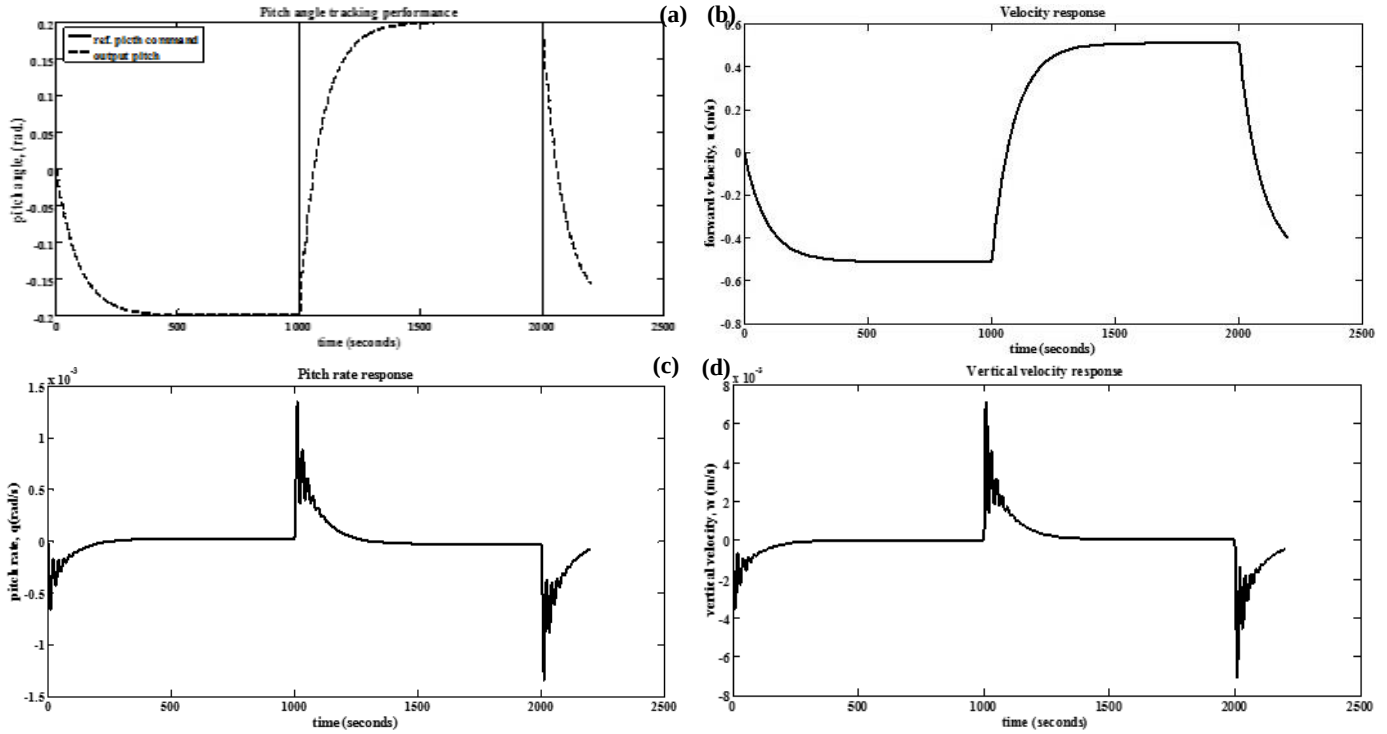

Figure 5 Responses to 0.2 rad square pitch command with nominal plant
(a) pitch angle, (b) forward velocity (c) pitch rate (d) vertical velocity

As indicated in Figure 5(a), the pitch angle command is effectively tracked with system settling time less than 450 seconds, approximately zero tracking error and minimal cross-coupling effect on off-axes responses. The robustness of

the compensator to sensor noise and disturbance input is obvious in the Figure 7. Compare to the magnitude of the disturbances as shown in the Figure 6, both the transient and steady state responses are not significantly affected. A steady state error of 0.0275 in the pitch angle is recorded compare to the response with the nominal system, while the settling remains approximately the same.

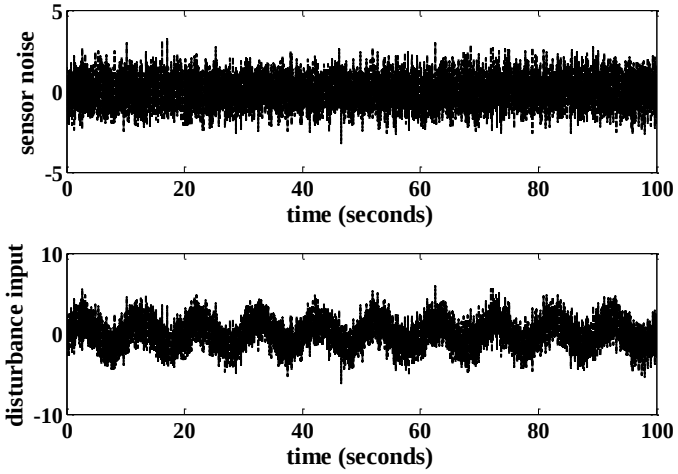

Figure 6 Sample sensor noise and input disturbance (0 to 100 s)

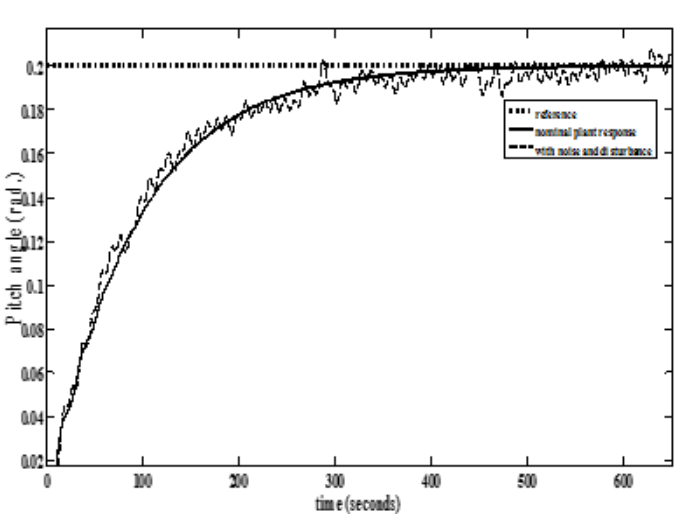

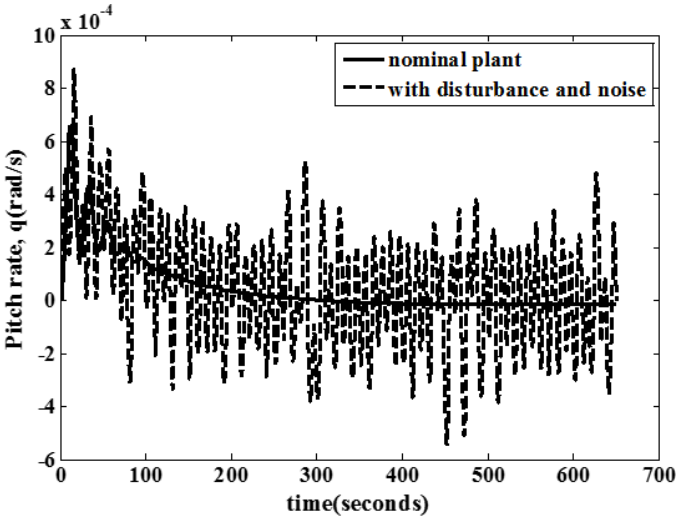

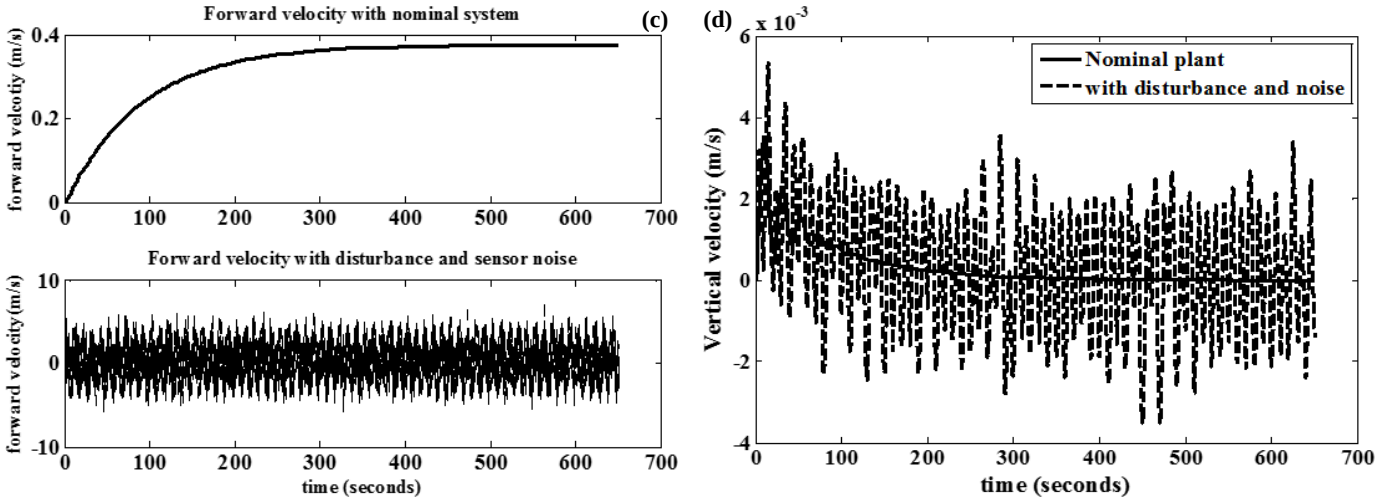

Figure 7 Responses to 0.2 rad step pitch command with and without disturbance and sensor noise: ***(a) pitch angle, (b) pitch rate, (c) forward velocity, and (d)*** **vertical velocity.**

V. CONCLUSIONS

The synthesis of an optimal LQR controller for a UUV system has been presented in this paper. The proposed design method utilizing a Pareto-based Multi-objectives differential evolution provides an automated and time saving design approach for such a complex dynamic system compare to the conventional method. The design method yields set of sub-optimal controller candidates, thereby provides insight into the performance interaction, and options to choose based on actual design goal. The analysis of the optimized LQR shows its effectiveness in both tracking and robust performances in the present of both sensor noise and disturbance input. Although, the problem in this study is formulated as a non-constraint optimization problem, the design algorithm is capable of accommodating additional constraints such as stability margin for a specific design scenario. This proposed automated controller synthesis is expected to facilitate the rapid prototyping and development of guidance and control algorithm for the unmanned underwater vehicle applications.

REFERENCES

[1] Ura T., AUV 'r2D4', Its Operation, and Road Map for AUV Development, in: *Advances in Unmanned Marine Vehicles*,edited by G.N. Roberts & R. Sutton, (IEE Control Series 69) 2006.

[2] A. Budiyono, Muljowidodo and A. Sugama, "Coefficient Diagram Method for the Control of an Unmanned Underwater Vehicle," *Indian J Mar Sci*., **38**(3):316-323, Sept. 2009

[3] R. K. Lea, R. Allen and S. L.Merry, "A comparative study of control techniques for an underwater flight vehicle," *International Journal of Systems Science*, volume 30, number 9, 1999, pp. 947- 964. CrossRef

[4] Agus Budiyono, "Advances in unmanned underwater vehicles technologies: Modeling, control and guidance perspectives', Indian J. of Geo-Marine Sciences, October 2009.

[5] Herman, P., Decoupled PD set-point controller for underwater vehicles. *Ocean Engineering*, 2009, vol. 36, no. 6-7, p. 529 to 534.

[6] Wei YH, Peng FG, Sheng C, et al. Control method of the stability of AUV. J Huazhong Univ Sci Technol Nat Sci Ed 2014; 42: 127–132.

[7] Rodrigues, L., Tavares, P., Prado, M. Sliding mode control of an AUV in the diving and steering planes. In *Proceedings of the MTS/IEEE Oceans'06 Conference*. FortLauderdale (FL, USA), 1996, p. 576 - 583. CrossRef

[8] Sabiha A Wadoo, Sadiksha Sapkota, Keerthish Chagachagere, "Optimal Control of an Autonomous Underwater Vehicle', Systems, applications and technology conference (LISAT), 4 May, 2012, IEEE Long Island.

[9] Field, A. I., Cherches, D., Calisal, S. Optimal control of an autonomous underwater vehicle. In *Proceedings of the World Automatic Congress*. Hawaii (USA), 2000, vol. 1, no. 38.

[10] Lin-LinWang,Hong-JianWang, and Li-Xin Pan. 'H∞ control for path tracking of autonomous underwater vehicle motion, Advances in Mechanical Engineering2015, Vol. 7(5) 1–18.

[11] Triantafyllou M.S. & Grosenbaugh M.A., Robust Control for Underwater Vehicle Systems with Time Delays, *IEEE Journal of Oceanic Engineering*, 16(1991) 146-151. CrossRef

[12] Yuh J., A Neural Net Controller For Underwater Robotic Vehicles, *IEEE Journal of Oceanic Engineering*, 15 (1990), 161-166. CrossRef

[13] Craven, P. J. (1999). Intelligent control strategies for an autonomous underwater vehicle. *PhD Thesis,University of Plymouth, UK.* CrossRef

[14] Ishii K., Fujii T. & Ura T., *Neural network system for online controller adaptation and its application to underwater robot*, (Proceedings of IEEE International Conference on Robotics & Automation) 1998, pp. 756–761. CrossRef

[15] M. Castillo-Effen, C. Castillo, W. Moreno, K. P. Valavanis, (2007). "Control Fundamentals of Small /Miniature Helicopters - A Survey". *Kimon P. Valavanis (ed.), Advances in Unmanned Aerial Vehicles, 73-118.* © 2007 *Springer. Printed in the Netherlands.* CrossRef

[16] W. Alvis, C. Castillo, M. Castillo-Effen, W. Moreno, K. P. Valavanis, (2007) "A Tutorial Approach to Small Unmanned Helicopter Controller Design for Nonaggressive Flights" Kimon P. Valavanis (ed.), Advances in Unmanned Aerial Vehicles, 119–170. © 2007 Springer. Printed in the Netherlands.

[17] Brian L. Stevens and Frank L. Lewis, (1992). Aircraft control and simulation, John Wiley & Sons, Inc.

[18] Ismaila B. Tijani, Rini Akmeliawati, Ari Legowo and **A. G. Abdul Muthalif, 2011.** Optimized LQR Control For 3DOF Helicopter Using Multiobjective Differential Evolution (Mode), in Computational Intelligent in Robust Control, IIUM Press.

[19] Tijani I.B.. Flight control system with MODE based H-infinity for small scale autonomous helicopter. PhD thesis submitted to Mechatronics engineering department, IIUM,Malaysia, October 2012.

[20] Ismaila B. Tijani, Rini Akmeliawati, Ari Legowo and Agus Budiyono**, (2015). "**Optimization of H-infinity Controller for Unmanned helicopter control using Pareto-based Multiobjective Differential Evolution.**"** Journal of Aerospace Engineering and Aircraft Technology, (AEAT).

[21] Muljowidodo, Jenie S.D., Budiyono A. & Adinugroho S., Design, Development and Testing of Underwater Vehicles: ITB Experience, paper presented at *The International Conference on Underwater System Technology: Theory and Application*, Penang, Malaysia, 2006.

[22] Storn, R. and Price, K.. Differential Evolution – A Simple and Efficient Heuristic for Global Optimization over Continuous Spaces, Journal of Global Optimization 11: 341–359, 1997, 341 1997 Kluwer Academic Publishers, 1997.

[23] Bourhane Kadmiry, (2002), 'Fuzzy Control for an Unmanned Helicopter', PhD thesis, Linköping Studies in Science and Technology, Department of Computer and Information Science, Linköpings Universitet, SE-581, 83 Linköping, Sweden